A&A 496, 429–439 (2009)
DOI: 10.1051/0004-6361:200810891

Astronomy & Astrophysics

The origin of abundance gradients in the Milky Way: the predictions of different models

E. Colavitti[1], G. Cescutti[1], F. Matteucci[1,2], and G. Murante[3]

[1] Dipartimento di Astronomia, Universitá di Trieste, via G. B. Tiepolo 11, 34143 Trieste (TS), Italy
e-mail: colavitti@oats.inaf.it
[2] INAF Osservatorio Astronomico di Trieste, via G. B. Tiepolo 11, 34143 Trieste (TS), Italy
[3] INAF Osservatorio Astronomico di Torino, Strada Osservatorio 20, 10025 Pino Torinese (TO), Italy

Received 27 August 2008 / Accepted 18 November 2008

ABSTRACT

Aims. We aim to study the abundance gradients along the Galactic disk and their dependence upon several parameters: a threshold in the surface gas density regulating star formation, the star formation efficiency, the timescale for the formation of the thin disk, and the total surface mass density of the stellar halo. We use chemical evolution models that already have been tested on a large number of observational constraints.

Methods. We test a model that considers a cosmological infall law. This law does not predict inside-out disk formation, but does allow the properties of the solar vicinity to be reproduced well. To check whether this model can reproduce the properties of the galactic disk, we study several cases. We lower the threshold of the surface gas density and assume that the star formation efficiency varies with radius. We test the same parameters in the two-infall model for the Galaxy. Finally, we complete some additional analyses of our simulations to test whether the cosmological infall law can account for the inside-out formation of the disk.

Results. We find that to reproduce simultaneously the abundance, star formation rate and surface gas density gradients along the Galactic disk it is necessary to assume that inside-out disk formation occurs. The threshold of the gas density is unnecessary and a similar effect could be achieved by assuming a variable star formation efficiency. The derived new cosmological infall law contains a mild inside-out formation and is still unable to reproduce the disk properties.

Conclusions. A cosmologically derived infall law with an inside-out process of disk formation and variable star formation efficiency can indeed reproduce well all the properties of the disk. However, the cosmological model presented here is of insufficient resolution to simulate accurately the inside-out formation for the disk. High resolution cosmological simulations should be performed to reproduce this behavior more accurately.

Key words. Galaxy: evolution – Galaxy: formation – Galaxy: disk – Galaxy: abundances

1. Introduction

Understanding the formation and the evolution of the Milky Way is fundamental to improving our knowledge in general of the formation of spiral galaxies. In many models of the chemical evolution of the Milky Way, gas infall has been invoked to explain the formation of the Galactic disk (e.g. Chiosi 1980; Lacey & Fall 1985; Matteucci & François 1989; Chiappini et al. 1997, hereafter C97); Boissier & Prantzos 2000; Portinari & Chiosi 2000, among others). Originally, gas infall was introduced as a possible solution of the G-dwarf problem (Pagel 1989). The infall law is clearly important to determining the main characteristics of a galaxy.

Our Galaxy has many observational constraints. Some of the most important ones are represented by the evolution in the chemical element abundances. Many chemical evolution models have been developed to explain the chemical composition of the solar vicinity (e.g. Henry et al. 2000; Liang et al. 2001; Chiappini et al. 2003a,b; Akerman et al. 2004; François et al. 2004; Cescutti et al. 2006, 2007). Other important constraints are the abundance gradients of the elements along the disk of the Milky Way. Abundance gradients are observed in many galaxies with their metallicities decreasing outward from the galactic centres. They are strongly influenced by both the star formation and the accretion history, because they are functions of galactocentric distance (see Matteucci & François 1989; Boissier & Prantzos 1999; Chiappini et al. 2001; Colavitti et al. 2008). Colavitti et al. (2008, hereafter C08), in particular, adopted a cosmologically motivated infall law, that assumed an accretion law for baryons similar to the accretion law of dark matter, obtained with the cosmological simulation public tree-code GADGET2 (Springel 2005). This cosmological law is able to reproduce well all the constraints in the solar vicinity, such as the star formation rate, the supernova (SN) Ia and SNII rate, the total amount of gas and stars, and the behavior of several chemical elements (such as the α-elements, C, N, and Fe).

We base our study in this paper on two chemical evolution models: the one of C97 and that of C08. The C08 model does not predict inside-out formation of the thin disk as in the C97 model, and while the C08 model predicts robustly the star formation rate and gas density distributions as functions of galactocentric distance, it does predict too flat a slope for the oxygen abundance gradient in the inner disk regions.

We attempt to test the predictions of the C08 model along the disk of the Milky Way by varying a number of important parameters to understand if there are alternative solutions to the inside-out formation and to the threshold in the gas density to reproduce abundance gradients. In particular, we test several cases in which we vary: i) the threshold gas density during the formation of the halo and thick and thin disk components; ii) the

efficiency of star formation as a function of galactocentric distance; iii) the total surface mass density of the stellar halo; and iv) the timescale for the formation of the thin disk. We do not test the effects of a variable initial mass function (IMF) along the disk, since this test has already been performed, and it has been concluded that it cannot reproduce simultanously the abundance gradients, the gas, and the star formation rate distributions (e.g. Carigi 1996; Chiappini et al. 2001). Radial flows can also play a role in the formation of abundance gradients (see Portinari & Chiosi 2000, and references therein). In particular, radial flows can produce gradients but mainly in the outer regions of the disk, while the inner gradients remain too flat. This effect is similar to that of varying the threshold in the gas density in the absence of an inside-out formation and therefore it is not accounted here. The effect produced by a bar in the bulge is more important since this is able to explain the peak of gas observed at 4–5 kpc from the Galactic center (Portinari & Chiosi 2000), in contrast to models that do not include the bar. However, we are uninterested in this problem but interested instead in the gradients and gas and star formation rate distributions for a galactocentric distance of $R_G > 4$ kpc.

We compare our model predictions with observational data that concerns in particular the abundance gradients along the disk, i.e. the data of Andrievsky et al. (2002a–c, 2004) and Luck et al. (2003). They measured the abundances of all selected elements (O, N, and Fe) in a sample of 130 Galactic Cepheids found in the Galactocentric distance range of between 5 and 17 kpc. Moreover, we compare our results with observational data collected by Simpson et al. (1995), Afflerbach et al. (1997), and Gummersbach et al. (1998) of the N gradient derived from HII regions, and with those collected by Chen et al. (2003), Twarog et al. (1997), and Carraro et al. (1998) for the Fe gradient measured for open clusters. We also compare our model results with measurements of star formation rate and surface gas density as functions of the Galactocentric distance by adopting the data collected by Rana (1991); this author considered the average of the *HI* distributions of Blitz et al. (1983), Gordon & Burton (1976), and Garwood & Dickey (1989) and two distinct H_2 distributions: one from Bronfman (1986) and the other from Robinson et al. (1988), Wouterloot et al. (1990), and Digel et al. (1990). Moreover, he considered the radial dependence of the present surface density of the star formation rate adopted from Rana & Wilkinson (1986).

The paper is organized as follows: in Sect. 2, we present the observational data and nucleosynthesis prescriptions adopted. Section 3 presents a briefly describes the model by C97. In Sect. 4, we describe the C08 model and the cosmological simulations. Section 5 describes the results obtained and compares the model predictions with the observed properties. Finally Sect. 6 presents the conclusions.

2. Observational data and nucleosynthesis prescriptions

We use the data of Luck et al. (2003) and Andrievsky et al. (2002a-c, 2004) for all studied chemical element abundance gradients. These data were derived for a large sample of Galactic Cepheids. These variable stars have a distinct role in determining radial abundance gradients for several reasons. First, they are usually sufficiently bright to be observed at large distances, providing accurate abundances; second, their distances are generally well determined, since these objects are often used as distance calibrators; third, their ages are also well determined. They generally have ages close to a few hundred million years, and we therefore can assume that they are representative of present day gradients.

We also use data from Gummersbach et al. (1998, B stars), Simpson et al. (1995) and Afflerbach et al. (1997) for HII regions, and Chen et al. (2003), Carraro et al. (1998) and Twarog et al. (1997) for open clusters.

One of the most important ingredients for chemical evolution models is represented by the nucleosynthesis prescriptions and, consequently, by stellar yields.

The single stars in the mass range $0.8\ M_\odot \leq M \leq 8\ M_\odot$ (low and intermediate-mass stars) contribute to Galactic enrichment through planetary nebula ejection and quiescent mass loss. They enrich the interstellar medium mainly in He, C, N, and heavy s-process elements (e.g. Cescutti et al. 2006). We adopt here the stellar yields for low and intermediate mass stars calculated by van den Hoek & Groenewegen (1997), which were computed as functions of stellar metallicity, in their case with variable mass loss. Concerning N production, the yields of van den Hoek & Groenewegen (1997) from AGB stars accounted for both primary and secondary N. For N produced in massive stars, we assume that it is secondary, although massive stars might produce primary nitrogen (e.g. Meynet & Maeder 2002) A small fraction of these stars are also the progenitors of type Ia SNe if they are in binary systems, which originate from carbon deflagration of C-O white dwarfs. In this paper, we adopt the single-degenerate progenitor scenario (Whelan & Iben 1973; Han & Podsiadlowski 2004). type Ia SNe contribute a substantial amount of Fe (~0.6 $M_\odot$ per event) and Fe-peak elements as well as non negligible quantities of Si and S. They also produce other elements, such as O, C, Ne, Ca, Mg, and Ni, although in small amounts compared to type II SNe. We assume the stellar yields of Type Ia SNe computed by Iwamoto et al. (1999).

Massive stars ($8\ M_\odot < M \leq 100\ M_\odot$) are the progenitor of core-collapse SNe, which can be either type II SNe or type Ib/c SNe. This latter type of supernova can arise either in binary systems or Wolf-Rayet stars, whereas type II SNe originate in massive stars in the lower mass range (Calura & Matteucci 2006). type II SNe mainly produce the so-called α-elements, such as O, Mg, Ne, Ca, S, Si, and Ti, but also some Fe and Fe-peak elements, although in smaller quantities than type Ia SNe. We adopt the stellar yields for massive stars evaluated by Woosley & Weaver (1995) with the suggested modifications of François et al. (2004). However, the most important modifications concern some Fe-peak elements, apart form Fe itself in contrast for the α-elements, with the exception of Mg which has been increased relative to the original yields, the yields are substantially unmodified relative to those of Woosley & Weaver's (1995). The reference solar abundances are those by Asplund et al. (2005).

3. The model by Chiappini et al. (1997)

The model by C97 was the first in which two main infall episodes during the formation of the Galactic components were suggested. In particular, they assumed that the first infall episode was responsible for the formation of the halo and thick-disk stars that originated from a rapid dissipative collapse. The second infall episode formed the thin-disk component, on a timescale far longer than that of the thick-disk formation. The timescale for the formation of the halo and thick disk is 0.8 Gyr, while the timescale for the thin disk is 7 Gyr in the solar vicinity. The authors also included in the model a threshold in the gas density, below which the star formation process ceases. The existence of such a threshold value was supported by observation measurements of the star formation in external disk galaxies

(Kennicutt 1998, but see Boissier et al. 2006). The physical reason for a threshold in star formation is related to gravitational stability, according to which, below a critical density, the gas is stable against density condensations and, consequently, the star formation is suppressed. In the two-infall model, the halo and thick and thin disk evolutions occur at different rates independently, mostly as a result of different accretion rates. With these precise prescriptions, it is possible to reproduce the majority of the observed properties of the Milky Way, and this illustrates the importance of the choice of both accretion law for the gas and the star formation rate during the evolution of the Galaxy. Some of the most important observational constraints are represented by the various relations between the abundances of metals (C, N, α-elements, iron peak elements) as functions of the [Fe/H] abundance and by the G-dwarf metallicity distribution. In C97 the Galactic disk is approximated by a series of concentric annuli, 2 kpc wide, that do not exchange matter. In this model, the thin disk forms "inside-out", in the sense that it assumes that the timescale for disk formation increases with Galactocentric distance. This choice was dictated by the necessity of reproducing the abundance gradients along the Galactic disk. The SFR is a Schmidt (1955) law with a dependence on the surface gas density ($k = 1.5$, see Kennicutt 1998) and also on the total surface mass density (see Dopita & Ryder 1994). In particular, the SFR is based on the law originally suggested by Talbot & Arnett (1975) and then adopted by Chiosi (1980):

$$\psi(r,t) = \nu \left(\frac{\Sigma(r,t)\Sigma_{\rm gas}(r,t)}{\Sigma(r_\odot,t)^2} \right)^{(k-1)} \Sigma_{\rm gas}(r,t)^k \quad (1)$$

where t is the time and the constant ν is a sort of efficiency of the star formation process and is expressed in Gyr^{-1}: in particular, $\nu = 2\ \mathrm{Gyr}^{-1}$ for the halo and $1\ \mathrm{Gyr}^{-1}$ for the disk ($t \geq 1$ Gyr). The total surface mass density is represented by $\Sigma(r,t)$, where $\Sigma(r_\odot,t)$ is the total surface mass density at the solar position, assumed to be $r_\odot = 8$ kpc (Reid 1993). The quantity $\Sigma_{\rm gas}(r,t)$ represents the surface gas density and t represents the time. This choice of parameter values allows the model to reproduce well the observational constraints, particularly in the solar vicinity. The IMF is that of Scalo (1986) normalized over a mass range of 0.1–100 $M_\odot$, which is assumed to be constant in space and time. In this paper, we also adopt a simple Schmidt law where the SFR depends only on the surface gas density:

$$\psi(r,t) = \nu\, \Sigma_{\rm gas}(r,t)^k \quad (2)$$

where $k = 1.5$, and ν is proportional to $1/R$.

4. The model of Colavitti et al. (2008)

The model of C08 is almost identical to that of C97 but has an accretion law that is derived from cosmological simulations. In particular, we developed a dark matter-only cosmological simulation, using the public tree-code GADGET2 (Springel 2005), to produce and study dark matter halos within which spiral galaxies can form. Our simulated box has a length of 24 h^{-1} Mpc. We used 256^3 particles. We adopted the standard cosmological parameters from WMAP 3-years (Spergel et al. 2007), namely $\Omega_0 = 0.275$, $\Omega_\lambda = 0.725$, and $\Omega_{\rm b} = 0.041$. Each DM particle has a mass equal to $6.289 \times 10^7\ \mathrm{h}^{-1}\ M_\odot$, and the Plummer-equivalent softening length is set equal to $3.75\ \mathrm{h}^{-1}$ comoving kpc to redshift $z = 2$ and to $1.25\ \mathrm{h}^{-1}$ physical kpc since $z = 2$. We used the public package GRAFIC (Bertschinger 1995) to set up our initial conditions. The simulation was initiated at redshift $z = 20$ and 28 outputs were produced. We chose to use a large spread in redshift at the beginning, while in the last part of the simulation, where a small redshift interval corresponds to a long in time, the redshift intervals were smaller. We confirmed that the final mass function of DM halos and the power spectrum were in agreement with theoretical expectations.

We identified DM halos at redshift $z = 0$ using a standard friend-of-friends (F-o-F) algorithm, with a linking length of $l = 0.17$ mean (comoving) interparticle distance. After that, we determined the virial mass and radius for each DM halo, using the center of mass of each F-o-F group as a measure of the halo center. Here, we define the virial radius as the radius of the sphere within which the matter density contrast is $\delta \approx 100$ times the critical density, where δ given by the cosmological parameter of Navarro & Steinmetz (2000).

We then compiled the mass accretion history of our halos by analyzing the 28 sets of output data obtained from redshift $z = 9.0$ to $z = 0$. We identified all DM halos in each snapshot using the procedure described above, except for the fact that we used the redshift-dependent density contrast given by Bryan & Norman (1997) to define the virial radius as a function of z. At any output z_{i+1}, we identified all progenitors of our halos at redshift z_i. We defined a halo at redshift z_{i+1} to be a progenitor of one at z_i if at least 50% of its particles belonged to the candidate offspring (see e.g. Kauffmann 2001; Springel et al. 2001) for a discussion of this threshold). The mass accretion history is defined to be the mass of the main progenitor of the halo as a function of redshift. With the mass accretion histories, we were able to identify the redshift of formation (defined to be the epoch at which half of the mass of the forming halos were accreted) and the redshift at which each halo experienced its most recent major merger (defined to correspond to an increase of at least 25% in its mass with respect to the mass of its main progenitor in the previous redshift bin). To identify DM halos capable of hosting a spiral galaxy similar to the MW, we used selection criteria based on four different characteristics of the halos:

- mass between $5 \times 10^{11}\ M_\odot$ and $5 \times 10^{12}\ M_\odot$;
- spin parameter $\lambda > 0.04$;
- redshift of last major merger ($z_{\rm mm}$) higher than $z = 2.5$;
- redshift of formation (z_f) higher than $z = 1.0$.

In this paper, we use our most accurately calibrated cosmological halo which has the following characteristics:

- $M = 90.26 \times 10^{10}\ M_\odot$;
- $\lambda = 0.045$;
- $z_{\rm mm} = 5.00$;
- $1.50 < z_{\rm f} < 1.75$.

Assuming that the baryonic matter follows the same accretion pattern as the dark matter, and represents 19% (the cosmological baryon fraction) of all infalling matter, we obtained a final baryonic mass for the Galaxy of $1.7 \times 10^{11}\ M_\odot$. We assumed that the infall law derived has the same functional form for the entire Milky Way, but that the normalization constant varies between the different Galactic regions. In other words, the normalization constants were obtained by reproducing the current total surface mass density at any specific galactocentric distance.

5. Results

We tested several different models to understand whether it is possible to reproduce all the observed values well by varying four variables. We note that in C08 (Model C08) we found that our most accurately calibrated cosmological model was unable

Table 1. Models parameters.

Model	Threshold	ν (4–6–8–10–12–14 kpc)	τ	$\Sigma_{\rm halo}$	Infall law	SFR
C08	yes	const	/	/	cosmological	Eq. (1)
C97	yes	const	$1.03 \cdot R$ - 1.27	const	two-infall law	Eq. (1)
1	no	const	/	/	cosmological	Eq. (1)
2	no	8.0–4.0–1.0–0.5–0.2–0.05	/	/	cosmological	Eq. (1)
3	no	4.0–1.0–0.1	/	/	cosmological with inside-out	Eq. (1)
4	no	const	const	const	two-infall law	Eq. (1)
5	no	const	$1.03 \cdot R$–1.27	const	two-infall law	Eq. (1)
6	no	9.0–3.0–1.0–0.3–0.1–0.03	$1.03 \cdot R$–1.27	$\propto 1/R$	two-infall law	Eq. (1)
7	no	$0.1 \cdot 8/R$	const	/	one-infall law	Eq. (2)

The second column indicates the presence or absence of a threshold, the third column the type of SF efficiency, the fourth whether the galaxy forms inside-out and the fifth whether the halo density is a constant or a function of radius. In the sixth column, we show the type of infall law used, and in the seventh column the SFR. The values of ν for Model 3 are for 2.5, 7.5, and 12.5 kpc.

to reproduce the [O/H] ratio in the inner Galactic disk. In this paper, we attempt to find a combination of variables that are able to reproduce the oxygen gradient more successfully. We also test these variables in the model by C97. We considered the following variables:

- **Threshold**. In the original model by C97, the threshold in the surface gas density equaled to 4 $M_\odot$ pc^{-2} during the formation of the halo, and 7 $M_\odot$ pc^{-2} during the formation of the thin disk. When the surface gas density was lower than these values the SFR stopped. In this paper, we do not apply the threshold in any of the models.
- **SF efficiency** (ν). In C97 and in C08, the star formation efficiency was assumed to be constant along the disk. Here we use, in some models, a SF efficiency that is a function of radius. This approach is already known (see Boissier & Prantzos 1999) and such a dependence has been proposed on the basis of large-scale instabilities in rotating discs. Even in Carigi (1996), the author used a model in which the star formation efficiency varied with radius ($\nu(r) \propto r^{-1}$, as already seen in Prantzos & Aubert 1995). We adopt several ad hoc variations of the parameter ν as a function of radius, in addition to the law adopted by Boissier & Prantzos (1999). All adopted laws are shown in Table 1.
- **Timescale for the formation of the disk** (τ). In C97, the Galactic disk forms inside-out. This implies that the inner parts of the Galactic disk form before than the outer parts. This type of formation was introduced to explain the measured Galactic gradients in chemical abundances. Even in Carigi (1996), the author used a model in which the infall timescale of the disk varied with radius. The model by C08, instead, did not adopt an inside-out scenario because the cosmologically derived infall law did not contain such a process. In this case, the parameter τ cannot therefore be changed. In Fig. 1, we show the cosmological infall law of C08 at different radii. The amount of gas infalling at each radii is clearly different, although the shape of the law remains unchanged. In some of the models, we used a constant timescale, while in others we used the prescription adopted in C97, namely:

$$\tau = 1.03\, r - 1.27 \text{ [Gyr]}, \quad (3)$$

where r is the galactocentric radius in kpc. Other authors also studied an inside-out formation of the disk by assuming a linear dependence of τ on r (e.g. Matteucci & François 1989; Carigi 1996; Boissier & Prantzos 1999).
- **Surface halo mass density** ($\Sigma_{\rm halo}$). In C97, the projected halo mass density was a constant parameter. Here, we use both a halo density that is a function of radius and a constant value, as in Chiappini et al. (2001), which follows the equation:

$$\Sigma_{\rm halo} = \frac{136}{r}\ \left[M_\odot \text{ pc}^{-2}\right], \quad (4)$$

where r is the radius in kpc. The value of 136 is adopted to ensure that the surface halo mass density equals 17 $M_\odot$ pc^{-2} in the solar neighbourhood. The halo density is important in determining the slope of the gradient at large galactocentric distances, where the disk density is low (see Chiappini et al. 2001).

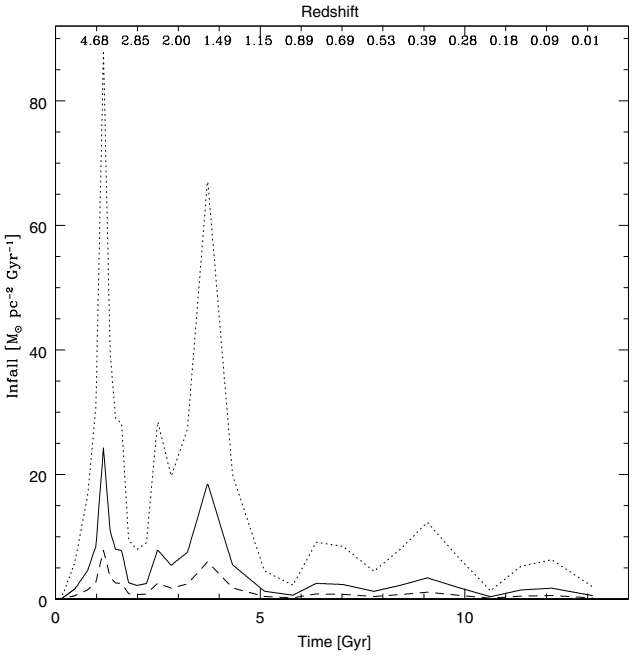

Fig. 1. Cosmological infall laws at Galactocentric radii of 4 kpc (blue dotted line), 8 kpc (red solid line), and 14 kpc (green dashed line).

In Table 1, we present both the models and all of the parameters that characterize them. The second column indicates the presence or absence of a threshold, the third column the type of variation in the SF efficiency (the values of ν in Model 3 are for 2.5, 7.5, and 12.5 kpc), the fourth indicates whether the galaxy forms inside-out or not, and the fifth whether the halo density is a constant or a function of radius. In the sixth column, we show the type of infall law used, and in the seventh column the SFR.

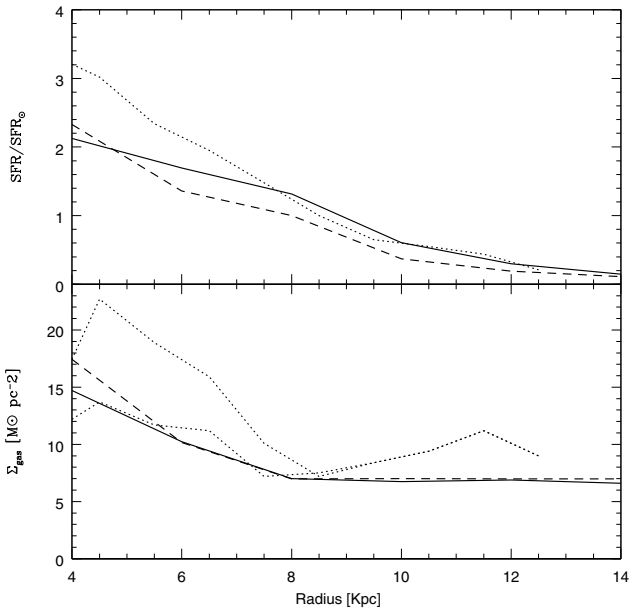

Fig. 2. $SFR/SFR_\odot$ and surface gas density versus radius for Model C97 (black solid line) and for Model C08 (red dashed line). The data are from Rana (1991, green dotted lines, representing the lower and the maximum values for the gas).

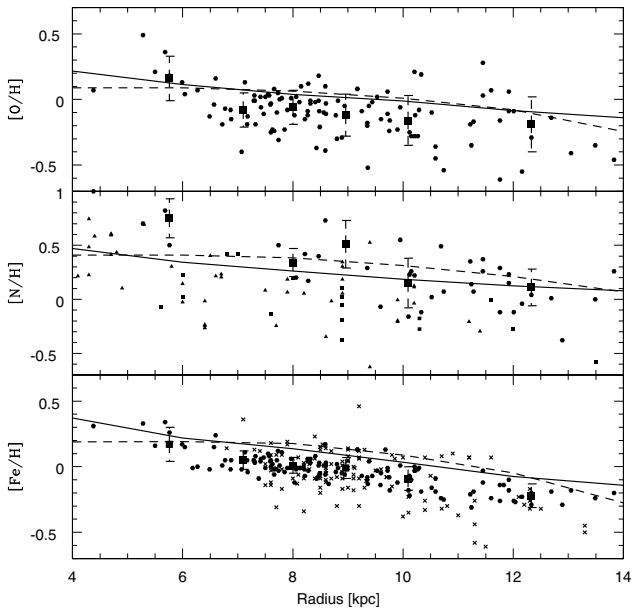

Fig. 3. [O/H], [N/H], and [Fe/H] versus radius for Model C97 (black solid line) and Model C08 (red dashed line). The data are from a compilation by Cescutti et al. (2007, blue dots, Cepheids), from Gummersbach et al. (1998, red squares, B stars), from Simpson et al. (1995) and Afflerbach et al. (1997, green triangles, HII regions), and from Chen et al. (2003), Carraro et al. (1998) and Twarog et al. (1997, cyan crosses, open clusters). The black squares are the mean values inside each bin only for the compilation by Cescutti et al. (2007) and the error bars represent their standard deviations.

Model C08 is the most accurately calibrated cosmological model of Colavitti et al. (2008). It assumes a threshold only during the formation of the disk, and a constant star formation efficiency ν. As explained above, with this model the authors were unable to reproduce the observed values of [O/H] in the inner part of the disk.

Model C97 is the original model of C97, i.e. the two-infall model. It has a threshold, both during the formation of the halo and thick-disk component and during the formation of the thin disk. Its star formation efficiency is constant with radius and equal to $\nu = 1.0$ Gyr^{-1}, and it has an inside-out prescription and a constant surface halo density along radius.

5.1. Results for models C08, C97, 1 and 2

In Figs. 2 and 3, we present the results for Model C97, compared with those predicted by Model C08 and observations. Figure 2, upper panel, presents the SFR normalized by the solar neighbourhood value. The data indicated by green dotted line are from Rana (1991), while the red dashed line represents Model C08. The black solid line represents Model C97. It can be seen that both Model C97 and Model C08 have no SF in the outer part of the disk, both having a threshold in the surface gas density below which SF ceases. The bottom panel of Fig. 2 shows the current surface gas density along the radius. The data are, once again, from Rana (1991). In this case, Model C97 and Model C08 produce very similar results. Moreover, both the models reproduce well the lower values of Rana (1991).

Figure 3 shows the evolution of [O/H], [N/H], and [Fe/H] with radius for Models C97 and C08. The model results are normalized to the values of the Asplund et al. (2005) solar abundances in all the models. The data are taken from a compilation by Cescutti et al. (2007, blue dots, Cepheids stars), from Gummersbach et al. (1998) (red squares, B stars), from Simpson et al. (1995) and Afflerbach et al. (1997) (green triangles, HII regions), and from Chen et al. (2003), Carraro et al. (1998) and Twarog et al. (1997) (cyan crosses, open clusters). The black squares are the mean values inside each bin only for the compilation by Cescutti et al. (2007), and the error bars are their standard deviations. It can be seen that Model C97 reproduces the data quite well, even in the inner part of the disk, since its slope is steeper than that of Model C08. As already said, the slope of Model C08 is too flat in the inner part of the disk. For this reason, we test several parameters in attempting to reproduce the inner abundance gradients. In the outer parts of the galactic disk, the slope of Model C08 is steeper than that of Model C97.

Figures 4 and 5 show the results for Model 1, which are compared with those predicted by Model C08 and observations. Model 1 is equivalent to Model C08, apart from the absence of threshold. We can see that Model 1 reproduces $SFR/SFR_\odot$ very well, far more closely than Model C08. However, Model 1 is unable to reproduce the surface gas density in the outer parts of the disk, since the obtained values are too low with respect to the observed values.

Figure 5 shows the abundance gradients for Model 1, compared with the results of Model C08. The data are the same as in Fig. 3. In this case, the absence of a threshold in the surface gas density causes the abundance gradients to be completely flat. Therefore, by simply removing the threshold from Model C08, we are unable to reproduce the chemical abundances in the direction of the galactic disk, either in the inner or outer parts. In the next model (Model 2), we therefore also use a star formation efficiency variable with radius.

In Figs. 6 and 7, the results obtained for Model 2, compared with those predicted by Model C08 and observations, can be seen. Model 2 assumes the same infall as Model C08 but has no threshold during the formation of the galactic disk. Moreover, in Model 2, we use a star formation efficiency, which is a function of radius.

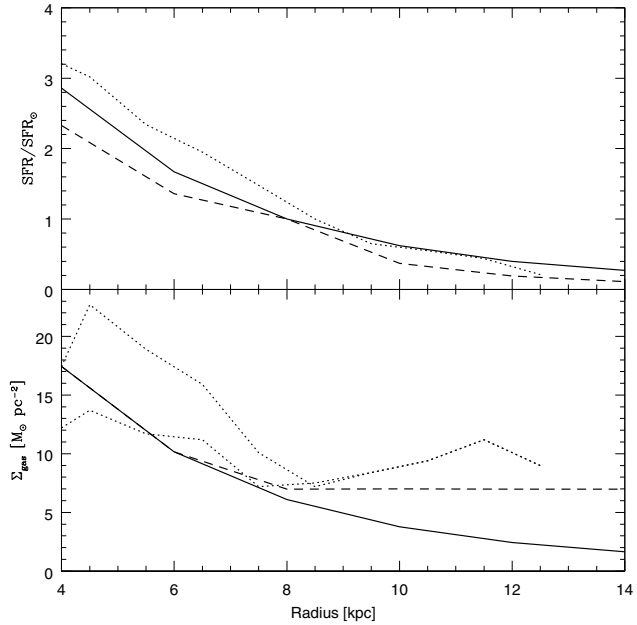

Fig. 4. $SFR/SFR_{\odot}$ and surface gas density versus radius in Model 1 (black solid line) and Model C08 (red dashed line). The data are the same as in Fig. 2.

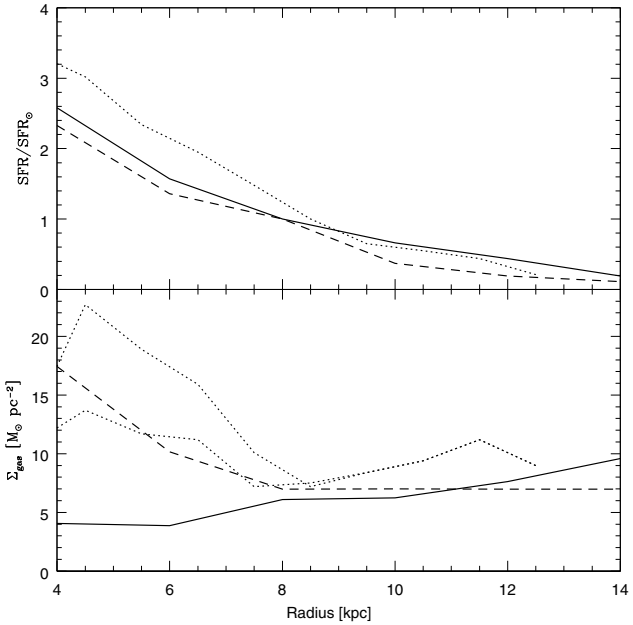

Fig. 6. $SFR/SFR_{\odot}$ and surface gas density versus radius in Model 2 (black solid line) and Model C08 (red dashed line). The data are the same as in Fig. 2.

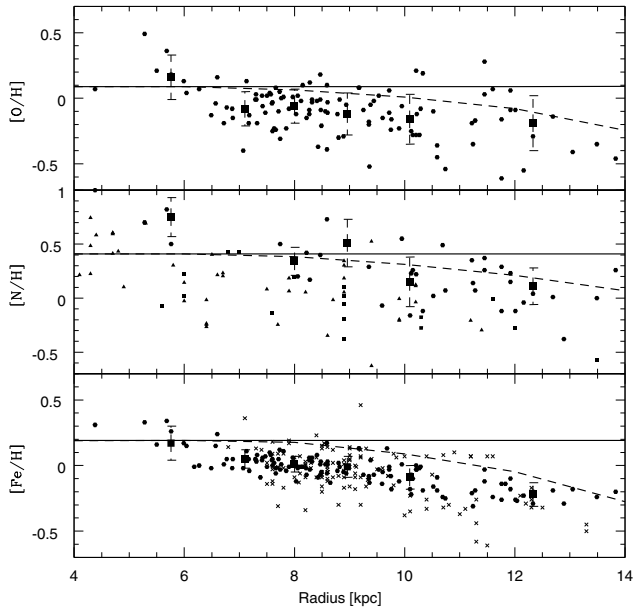

Fig. 5. [O/H], [N/H], and [Fe/H] versus radius in Model 1 (black solid line) and Model C08 (red dashed line). The data are the same as in Fig. 3.

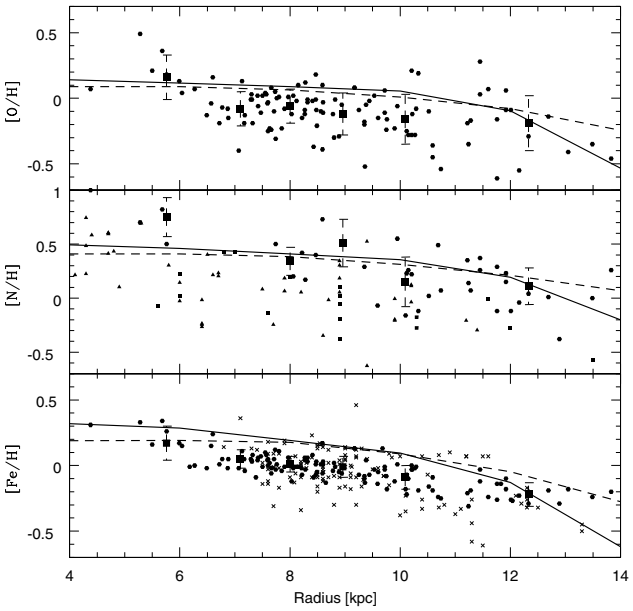

Fig. 7. [O/H], [N/H] and [Fe/H] versus radius in Model 2 (black solid line) and Model C08 (red dashed line). The data are the same as in Fig. 3.

In the upper panel of Fig. 6, it can be seen that Model 2 is in closer agreement with the data than Model C08, especially in the outer part of the disk. Model C08 has a $SFR/SFR_{\odot}$ equal to zero in the outer parts of the disk, which is due to the presence of the threshold. From the bottom panel of Fig. 6 we can see that Model C08 is in quite good agreement with the data, whereas Model 2 predicts a surface gas density at variance with the observations: it predicts too low a surface gas density in the inner disk because of the high SF efficiency.

Figure 7 shows the evolution of [O/H], [N/H], and [Fe/H] as a function of radius for Models C08 and 2. Using no threshold and a star formation efficiency that varies with radius, we are again unable to reproduce, as we hoped, the gradients in the inner parts of the disk. We can only increase the slope of the gradients, relative to Model C08 in the outer parts.

Since we are unable simultaneously to reproduce well the surface gas density and the abundance gradients along the Galactic disk using the cosmologically derived infall law by C08 either without the threshold, or without the threshold and adopting a SF efficiency that varies with radius, we now attempt another approch. As we said in Sect. 4, model C08 assumed that the derived infall law has the same functional form for the entire Milky Way, but that the normalization constant differs between different Galactic regions.

5.2. Results for the cosmological infall law with inside-out

We then attempted to derive infall laws that had a different functional form along the disk. In achieving this, we divided the galactic disk into three zones. The first included the central 5 kpc of the disk, the second was a radial shell beginning at 5 kpc and ending at 10 kpc, and the third shell had an inner and outer radii of 10 and 15 kpc, respectively. With knowledge of the coordinates of each DM particle in the main progenitor at each redshift, we calculated the total mass included in each shell, by deriving three different cosmological infall laws in the three zones. It is well-known (Helmi et al. 2003, and references therein) that the build-up of a Galaxy-sized DM halo proceeds in an inside-out fashion, with the mass of the inner part of the halo being in place at high redshift, while its outer part continues to accrete mass until low redshift. We wished to determine whether a cosmological, standard-resolution simulation could still reproduce this behavior; we could then verify whether such a simulation could be used to develop a cosmological, inside-out, baryonic accretion law, without requiring higher resolution simulations of single halos to be completed with DM only or with more complex physics. It is also known that re-simulation of single halos, with gas physics, a star formation prescription, and some effective form of SN energy feedback can reproduce an inside-out formation of disk galaxies (Governato et al. 2007; Abadi et al. 2003a,b). Such numerical simulations are however computationally very expensive and the properties of the simulated galaxy somehow depend on the sub-grid prescription for the various astrophysical processes. Our aim here is to see whether we can obtain similar results using a much simpler numerical approach.

We then tested these laws in the chemical evolution model, using no threshold and a star formation efficiency that varies with radius. In Figs. 8 and 9, our results can be seen.

Figure 8 shows that Model 3 reproduces well the observed SFR, especially between 9 and 12.5 kpc. The slope of the curve of observable data is similar to that of Model 3. The predicted SFR is slightly higher than observed only at 2.5 kpc. However, the improvement with respect to model C08 is clear and it is mainly due to the lack of a threshold in the superficial gas density. In the bottom panel, it can be seen that Model 3 has too low a value of Σ_{gas} with respect to the observable data and model C08. However, it is interesting that the behavior of the curve is similar to that of the observable data since the increase in the superficial gas density observed by Rana (1991) in the outer part of the disk is also predicted by Model 3. Moreover, the value at 2.5 kpc equals that measured for the observable data.

Figure 9 shows the derived [O/H], [N/H], and [Fe/H] as a function of radius for Model 3. It can be seen that in the case of O and N the results are similar to those of model C08, even if the slope reproduced by Model 3 is steeper. The slope is clearly steeper for [Fe/H], especially in the outer part of the disk. However, not even Model 3 is able to reproduce the slope in the inner part of the Galaxy, in spite of the fact that the accretion law simulates an inside-out formation. This is due to the mildness of the inside-out formation predicted by the infall law, which can be attributed to the relatively low resolution that our cosmological simulation can achieve on a single halo, especially at high redshifts.

5.3. Varying the parameters in the C97 models

After this study of the cosmological model by C08, we considered the model by C97, in trying to find the optimal combination of parameters to reproduce the $SFR/SFR_{\odot}$, surface gas density

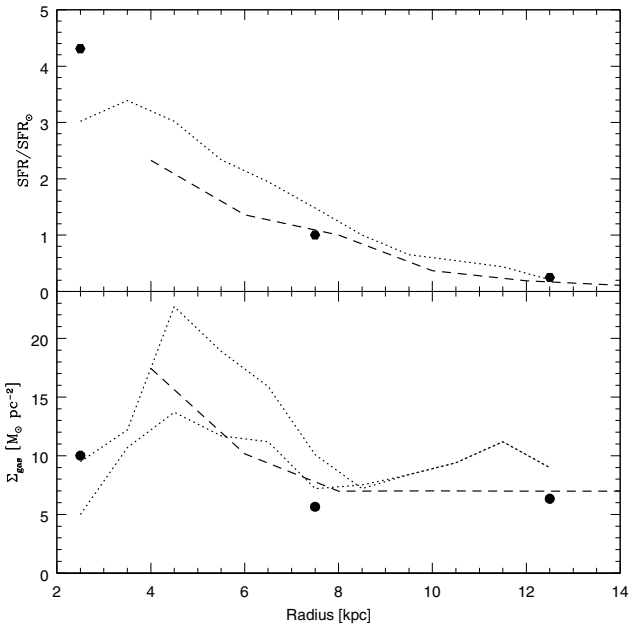

Fig. 8. $SFR/SFR_{\odot}$ and surface gas density versus radius in Model 3 (black points) and Model C08 (red dashed line). The data are the same as in Fig. 2.

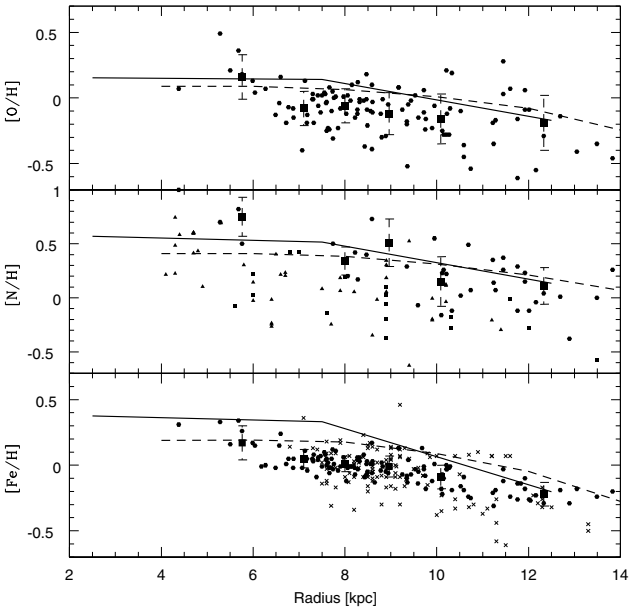

Fig. 9. [O/H], [N/H], and [Fe/H] versus radius in Model 3 (black solid line) and Model C08 (red dashed line). The data are the same as in Fig. 3.

and abundance gradients along the Galactic disk, as achieved for Model C08. In this case, we studied the behavior of the parameters in four different models, comparing every model with Model C08.

Figures 10 and 11 show the results for Model 4. This Model has no threshold and the SF efficiency ν, τn and Σ_{halo} are constants. In Fig. 10 it can be seen that the predicted star formation rate of Model 4 agrees well with the data by Rana (1991). However, Σ_{gas} is too low in the outer parts of the disk, even if in the inner parts it agrees well with the observed values.

Figure 11 shows [O/H], [N/H], and [Fe/H] as a function of radius for Model 4. We can see that in the inner disk the

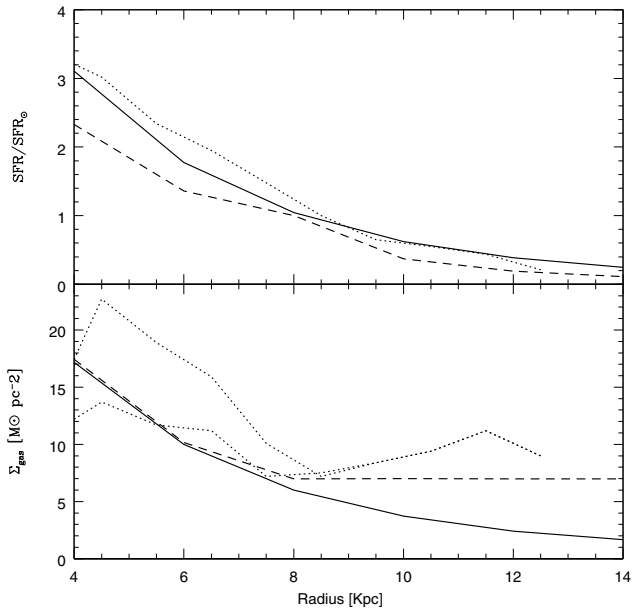

Fig. 10. $SFR/SFR_{\odot}$ and surface gas density versus radius in Model 4 (black solid line) and Model C08 (red dashed line). The data are the same as in Fig. 2.

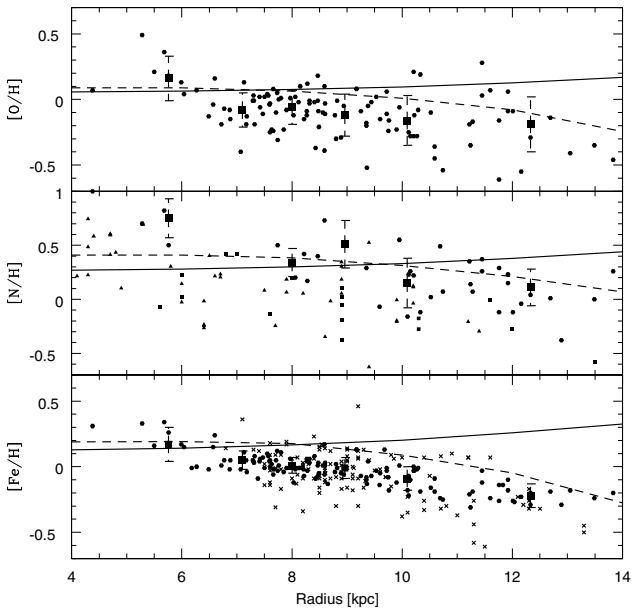

Fig. 11. [O/H], [N/H], and [Fe/H] versus radius in Model 4 (black solid line) and Model C08 (red dashed line). The data are the same as in Fig. 3. It can be seen that in the outer part of the disk the gradients become steeper. In fact, since the halo surface mass density is constant along the galactic disk and there is no threshold in the surface gas density, the star formation in the halo becomes more significant than that in the outer disk.

abundance gradients are flat, while in the outer parts they even increase, in contrast to the observed data. Therefore, it is impossible to reproduce the abundance gradients without threshold and when ν, τ and $\Sigma_{\rm halo}$ remain constant. This is because a constant τ causes disk evolution to proceed too rapidly for abundance gradients to form, such that the star formation never ceases (in the absence of a threshold) and the halo surface mass density is constant with galactocentric distance. In this case, the star formation in the halo, in fact, overwhelms that proceding in the outer disk and leading to higher abundances than in the more realistic case of a decreasing surface halo mass density.

Figures 12 and 13 compare Model 5 with Model C08. Model 5 has no threshold (either in the halo or in the disk), a constant star formation efficiency, a variable τ along the disk and a constant surface halo density. From Fig. 12 it can be seen that the star formation rate predicted by Model 5 agrees well with the data by Rana (1991), especially in the outer parts of the galaxy. However, the amount of gas predicted is too low, even when compared with the lower values of Rana (1991).

Figure 13 shows the abundance gradients along the galactic disk in Model 5. In the inner part of the disk, the [O/H], [N/H], and [Fe/H] ratios are not flat as in Model C08, reproducing the observed data more successfully. Nevertheless, beyond 10 kpc, the gradients become positive, at variance with the observations. So we can say that a model without a threshold and with a variable τ cannot well reproduce the data, especially in the outer disk.

Figures 14 and 15 show the $SFR/SFR_{\odot}$, $\Sigma_{\rm gas}$, and [O/H], [N/H], and [Fe/H] gradients for Model 6. This model has no threshold, a star formation efficiency that varies significantly with radius, an inside-out prescription, and a surface halo density that is a function of radius. From Fig. 14, it can be seen that the SFR is in good agreement with the data, especially in the outer parts of the disk. On the other hand, the surface gas density increases as a function of radius, at variance with the observations, which indicate that there is more gas in the inner parts of the disk.

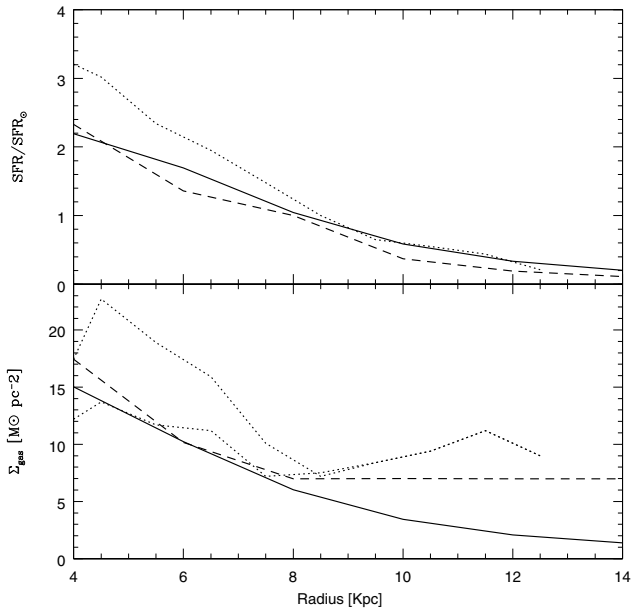

Fig. 12. $SFR/SFR_{\odot}$ and surface gas density versus radius in Model 5 (black solid line) and for Model C08 (red dashed line). The data are the same as in Fig. 2.

In Fig. 15, we can see that the abundance gradients have a slope that is similar to the slope in the data, mainly for the [Fe/H] ratio. Even in the inner parts of the Galaxy the gradients are in good agreement with the data. However, we are unable to say whether this model can reproduce all the observations, since it is unable to reproduce the correct behavior of $\Sigma_{\rm gas}$.

The last model that we present is Model 7. Its results are shown in Figs. 16 and 17. This model has no threshold, a star formation efficiency that follows the law adopted by

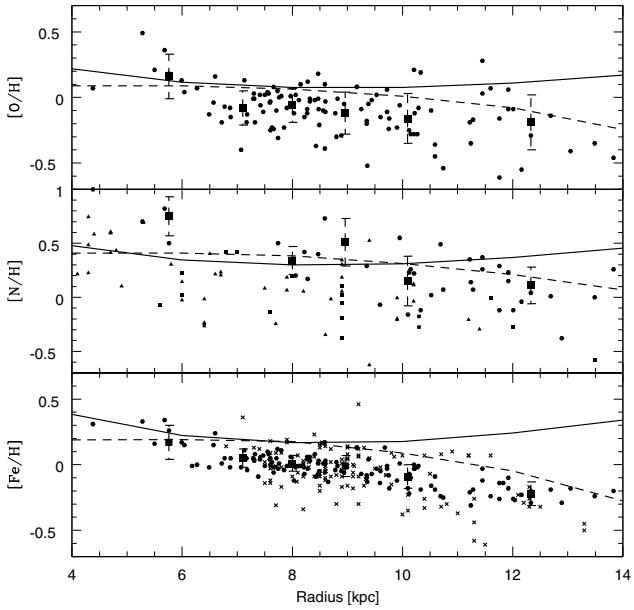

Fig. 13. [O/H], [N/H] and [Fe/H] versus radius in Model 5 (black solid line) and Model C08 (red dashed line). The data are the same as in Fig. 3. This model demonstrates a variable τ along the galactic disk causes the inner gradients to steepen, without the positive slope being reduced in the outer disk, as seen in Fig. 11.

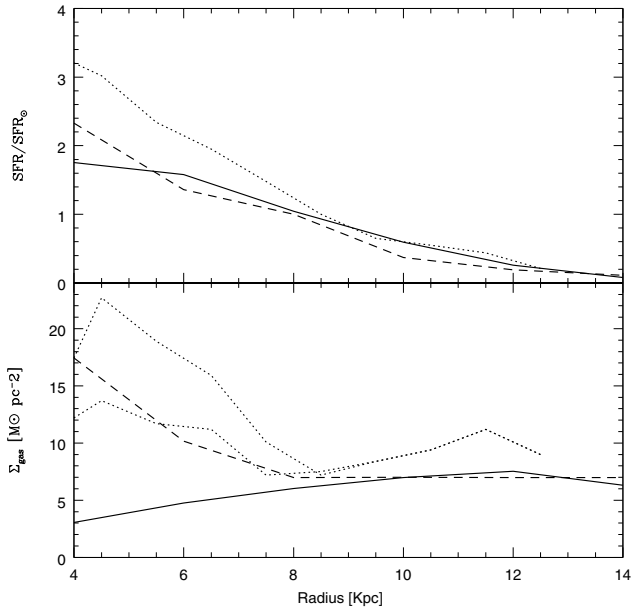

Fig. 14. $SFR/SFR_{\odot}$ and surface gas density versus radius in Model 6 (black solid line) and Model C08 (red dashed line). The data are the same as in Fig. 2.

Boissier & Prantzos (1999) and no inside-out prescription. In this model, we assume only one episode of accretion in which the halo forms first and then the disk follows. It also differs from all other models because it adopts a simple Schmidt law for star formation, as in Eq. (2). It can be seen that the SFR agrees well with the data by Rana (1991), while the surface gas density is too low in the inner part of the Galactic disk. This is again due to too high a SF efficiency in the inner disk.

From Fig. 17 we can see that Model 7 predicts abundance gradients that are in good agreement with the observed data, especially in the outer parts of the Galactic disk. We can

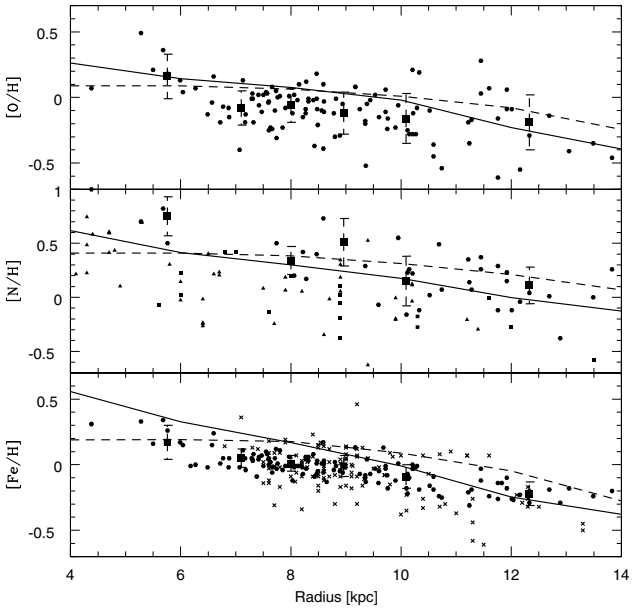

Fig. 15. [O/H], [N/H] and [Fe/H] versus radius in Model 6 (black solid line) and Model C08 (red dashed line). The data are the same as in Fig. 3.

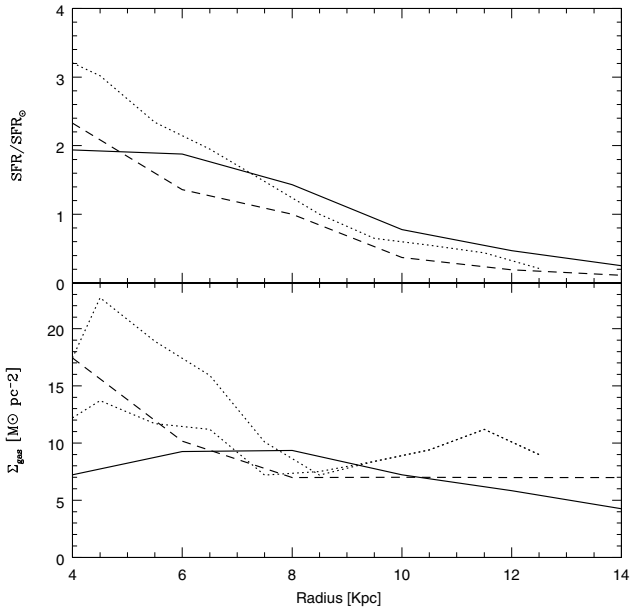

Fig. 16. $SFR/SFR_{\odot}$ and surface gas density versus radius in Model 7 (black solid line) and for Model C08 (red dashed line). The data are the same as in Fig. 2.

therefore say that this is the only case for both no threshold and no inside-out prescription where it is possible to reproduce abundance gradients well, although the surface gas density is too low in the inner part of the Galaxy.

6. Conclusions

We have tested several models to identify the optimal values of four parameters that enable the $SFR/SFR_{\odot}$, $\Sigma_{\rm gas}$, and the [O/H], [N/H], and [Fe/H] gradients along the Galactic disk, to be reproduced most successfully. We started from the model of Colavitti et al. (2008) and adopted a cosmologically-motivated infall law resembling that of C97 in the solar neighbourhood, which does

Table 2. Models successes and failures. The second column shows the successes, while the third column indicates the failures.

Model	Successes	Failures
1	good agreement for the $SFR/SFR_{\odot}$	Σ_{gas} not reproduced in the outer Galactic disk abundance gradients completely flat
2	good agreement for the $SFR/SFR_{\odot}$ increased slope of the gradients in the outer disk	too low Σ_{gas} in the inner disk abundance gradients too flat in the inner disk
3	good agreement for the $SFR/SFR_{\odot}$ Σ_{gas} increases in the outer part of the disk slope of abundance gradients more pronunced in the outer disk	too low Σ_{gas} abundance gradients too flat in the inner disk
4	good agreement for the $SFR/SFR_{\odot}$	Σ_{gas} not reproduced in the outer Galactic disk abundance gradients increase along the galactic disk
5	good agreement for the $SFR/SFR_{\odot}$ slope of abundance gradients more pronunced in the inner disk	Σ_{gas} not reproduced in the outer Galactic disk abundance gradients increase in the outer Galactic disk
6	good agreement for the $SFR/SFR_{\odot}$ abundance gradients in good agreement with the observed data	Σ_{gas} increases along radius
7	good agreement for the $SFR/SFR_{\odot}$ abundance gradients in good agreement with the observed data	Σ_{gas} too low in the inner part of the Galactic disk

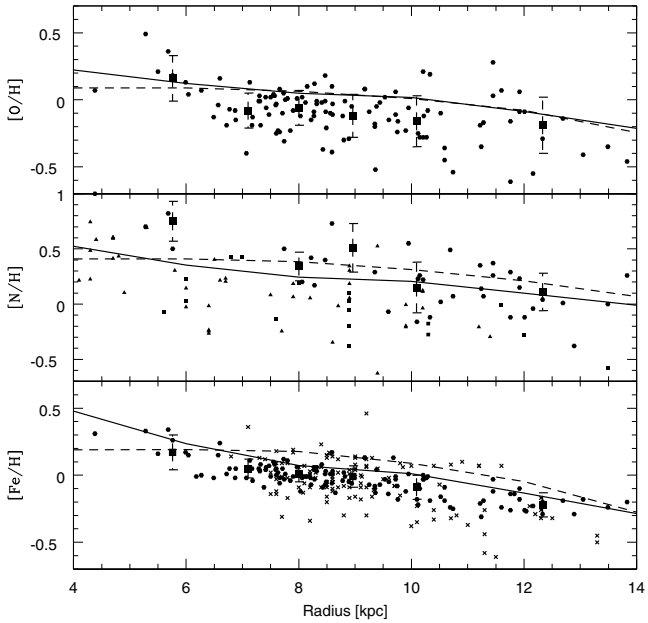

Fig. 17. [O/H], [N/H] and [Fe/H] versus radius in Model 7 (black solid line) and for Model C08 (red dashed line). The data are the same as in Fig. 3.

not however predict inside-out formation of the Galactic disk and did not enable the authors to reproduce the [O/H] gradient in the inner parts of the disk. These four parameters are the threshold gas density for the star formation, the star formation efficiency ν, the inside-out prescription $\tau(r)$ (i.e. the variation in the timescale of the formation of the Galactic disk) and the surface halo mass density.

In Table 2 we summarize the model successes and failures in terms of abundance trends, surface gas densities, and star formation rates.

Our conclusions can be summarized as follows:

- We have found that it is impossible to satisfy all the disk constraints simultaneously without assuming an inside-out formation for the Galactic disk and a threshold in the gas density for the star formation rate. In particular, the inside-out formation is important in reproducing the correct slope of the abundance gradients in the inner disk, whereas the threshold gas density is important to reproduce the slope of the gradients in the outer disk. Models with a constant timescale for disk formation (no inside-out process) cannot reproduce the slope in the inner disk. On the other hand, models with no inside-out mechanism can reproduce the distributions of the star formation rate and the gas density along the disk well. A good way of testing inside-out disk formation is to test whether there is a size and luminosity evolution in disks at high redshift. By studying galaxies in the redshift range 2.5–3.0, Roche et al. (1998) concluded that the larger increase in the surface brightness relative to the luminosity at high redshift is indicative of inside-out disk formation. They tested their results by means of the Chiappini et al. (1997) model. Another important issue concerns the existence of a threshold gas density for star formation. By means of GALEX data, Boissier et al. (2006) suggested that the threshold might not exist or be far lower than previously believed. We note, however, that the low level of star formation detected by GALEX in the outer edges of disks does not produce OB associations, hence no massive stars, which are the main contributors to the enrichment of the ISM. Therefore, the abundance gradients measure the threshold for massive star formation.
- In the framework of models with no inside-out mechanism such as the model proposed by Colavitti et al. (2008), we tested the effect of variations in the efficiency of star formation with the galactocentric radius, such that the efficiency was higher in the innermost parts than in the outermost regions of the Galactic disk. This assumption, even without the threshold in the surface gas density, can produce gradients of the correct slope both in the inner and outer regions of the Galactic disk but fails to reproduce the gas density distribution along the disk.
- A cosmological model without a threshold, and with a star formation efficiency that varies with radius and a simple inside-out prescription, can reproduce the SFR along the disk and the behavior of the surface gas density well. Moreover, it can reproduce the outer abundance gradients. In the inner part of the disk, it produces gradients that are too flat, even if the slope is steeper than for Model C08.
- Therefore, we conclude that to reproduce at the same time the abundance, star formation rate, and surface gas density gradients along the Galactic disk, it is necessary to assume

an inside-out formation for the disk. The threshold in the gas density is unnecessary, and the same effect could be reached by assuming a variable efficiency of star formation. The inclusion of radial flows without an inside-out formation of the disk would have the same effect as the theshold gas density without inside-out effect (Portinari & Chiosi 2000).

– It is clear from our numerical simulations that while the process of formation of the Galactic disk has a major impact on the formation of abundance gradients, the specific SF law adopted has a major effect on the gas distribution along the disk. This effect could be used to infer the SF law from the gas distributions along the disks of spirals.
– As far as the Colavitti et al. (2008) model is concerned, we conclude that our cosmological simulation has insufficient resolution to capture the inside-out formation of a galaxy-sized DM halo. Higher resolution cosmological simulations and/or resimulation of a single DM halo should be performed to understand if a suitable baryon accretion law can be inferred from collisionless simulations, or if the full gas physics and sub-grid treatment of astrophysical processes such as star formation and energy feedback from SNe, is definitely required to achieve a realistic description of the formation of a galaxy.

Acknowledgements. We thank Francesco Calura for some helpful suggestions. E.C. and F.M. aknowledge funds from MIUR, COFIN 2007, prot. N. 2007JJC53X. G.C. aknowledges financial support from the Fondazione Cassa di Risparmio di Trieste. We also thank the unknown referee for the suggestions.

References

Abadi, M. G., Navarro, J. F., Steinmetz, M., & Eke V. R. 2003a, ApJ, 591, 499
Abadi, M. G., Navarro, J. F., Steinmetz, M., & Eke, V. R. 2003b, ApJ, 597, 21
Afflerbach, A., Churchwell, E., & Werner, M. W. 1997, ApJ, 478, 190
Akerman, C. J., Carigi, L., Nissen, P. E., Pettini, M., & Asplund, M. 2004, A&A, 414, 931
Alibés, A., Labay, J., & Canal, R. 2001, A&A, 370, 1103
Andrievsky, S. M., Kovtyukh, V. V., Luck, R. E., et al. 2002a, A&A, 381, 32
Andrievsky, S. M., Bersier, D., Kovtyukh, V. V., et al. 2002b, A&A, 384, 140
Andrievsky, S. M., Kovtyukh, V. V., Luck, R. E., et al. 2002c, A&A, 392, 491
Andrievsky, S. M., Luck, R. E., Martin, P., et al. 2004, A&A, 413, 159
Asplund, M., Grevesse, N., & Sauval, A. J. 2005, ASPC, 336, 25
Bertschinger, E. 1995 [arXiv:astro.ph/9506070]
Blitz, L., Fich, M., & Kulkarni, S. 1983, Science, 220, 1233
Boissier, S., & Prantzos, N. 1999, MNRAS, 307, 857
Boissier, S., & Prantzos, N. 2000, MNRAS, 312, 398
Boissier, S., Gil de Paz, A., Boselli, A., et al. 2007, ApJS, 173, 524
Bronfman, L. 1986, Ph.D. Thesis Univ. Columbia, 251
Bryan, G. L., & Norman, M. L. 1997, ASPC, 123, 363
Calura, F., & Matteucci, F. 2006, ApJ, 652, 889
Carigi, L. 1996, Rev. Mex. Astron. Astrofis, 32, 179
Carraro, G., Ng, Y. K., & Portinari, L. 1998, MNRAS, 296, 1045
Cescutti, G., François, P., Matteucci, F., Cayrel, R., & Spite, M. 2006, A&A, 448, 557
Cescutti, G., Matteucci, F. François, P., & Chiappini, C. 2007, A&A, 462, 943
Chang, R. X., Hou, J. L., Shu, C. G., & Fu, C. Q. 1999, A&AS, 141, 491
Chen, L., Hou, J. L., & Wang, J. J. 2003, AJ, 125, 1397
Chiappini, C., Matteucci, F., & Gratton, R. 1997, ApJ, 477, 765
Chiappini, C., Matteucci, F., & Romano, D. 2001, ApJ, 554, 1044
Chiappini, C., Romano, D., & Matteucci, F. 2003a, MNRAS, 339, 63
Chiappini, C., Matteucci, F. & Meynet, G. 2003b, A&A, 410, 257
Chiosi, C. 1980, A&A, 83, 206
Colavitti, E., Matteucci, F., & Murante, G. 2008, A&A, 483, 401
Digel, S., Bally, J., & Thaddeus, P. 1990, ApJ, 357, 29
Dopita, M. A., & Ryder, S. D. 1994, ApJ, 430, 163
François, P., Matteucci, F., Cayrel, R., et al. 2004, A&A, 421, 613
Garwood, R. W., & Dickey, J. M. 1989, ApJ, 338, 841
Gordon, M. A., & Burton, W. B. 1976, ApJ, 208, 346
Governato, F., Willman, B., Mayer, L., et al. 2007, MNRAS, 374, 1479
Gummersbach, C. A., Kaufer, A., Schäfer, D. R., Szeifert, T., & Wolf, B. 1998, A&A, 338, 881
Han, Z., & Podsiadlowski, P. 2004, MNRAS, 350, 1301
Helmi, A., White, S. D. M., & Springel, V. 2003, MNRAS, 339, 834
Henry, R. B. C., Edmunds, M. G., & Köppen, J. 2000, ApJ, 541, 660
Hou, J. L., Prantzos, N., & Boissier, S. 2000, A&A, 362, 921
Kauffmann, G. 2001, ASPC, 245, 381
Kennicutt, R. C. Jr. 1998, AAR&A, 36, 189
Lacey, C. G., & Fall, S. M. 1985, ApJ, 290, 154
Liang, Y. C., Zhao, G., & Shi, J. R. 2001, A&A, 374, 936
Luck, R. E., Gieren, W. P., Andrievsky, S. M., et al. 2003, A&A, 401, 939
Matteucci, F., & François, P. 1989, MNRAS, 239, 885
Meynet, G., & Maeder, A. 2002, A&A, 381, 25
Navarro, J. F., & Steinmetz, M. 2000, ApJ, 538, 477
Portinari, L., & Chiosi, C. 2000, A&A, 355, 929
Prantzos, N., & Aubert, O. 1995, A&A, 302, 69
Rana, N. C. 1991, ARA&A, 29, 129
Rana, N. C., & Wilkinson, D. A. 1986, MNRAS, 218, 721
Reid, M. J. 1993, ARA&A, 31, 345
Robinson, B. J., Manchester, R. N., Whiteoak, J. B., Otrupcek, R. E., & McCutcheon, W. H. 1988, A&A, 193, 60
Roche, N., Ratnatunga, K., Griffiths, R. E., Im, M., & Naim, A. 1998, MNRAS, 293, 157
Scalo, J. M. 1986, FCPh, 11, 1
Simpson, J. P., Colgan, S. W. J., Rubin, R. H., Erikson, E. F., & Haas, M. R. 1995, ApJ, 444, 721
Spergel, D. N., Bean, R., Dor, O., et al. 2007, ApJS, 170, 377
Springel, V. 2005, MNRAS, 364, 1105
Springel, V., White, S. D. M., Tormen, G., & Kauffmann, G. 2001, MNRAS, 328, 726
Talbot, R. J. Jr., & Arnett, W. D. 1975, ApJ, 197, 551
Twarog, B. A., Ashman, K. M., & Anthony-Twarog, B. J. 1997, ApJ, 114, 2556
van den Hoek, L. B., & Groenewegen, M. A. T. 1997, A&AS, 123, 305
Whelan, J., & Iben, I. Jr. 1973, ApJ, 186, 1007
Woosley, S. E., & Weaver, T. A. 1995, AIPC, 327, 365
Wouterloot, J. G. A., Brand, J., Burton, W. B., & Kwee, K. K. 1990, A&A, 230, 21